Neurosci. Bull. October, 2022, 38(10):1183–1198
https://doi.org/10.1007/s12264-022-00884-z

www.neurosci.cn
www.springer.com/12264

ORIGINAL ARTICLE

Modulation of Neuronal Activity and Saccades at Theta Rhythm During Visual Search in Non-human Primates

Jin Xie[1,2] · Ting Yan[1] · Jie Zhang[1,2,3] · Zhengyu Ma[3] · Huihui Zhou[1,3]

Received: 12 November 2021 / Accepted: 18 March 2022 / Published online: 24 May 2022

Abstract Active exploratory behaviors have often been associated with theta oscillations in rodents, while theta oscillations during active exploration in non-human primates are still not well understood. We recorded neural activities in the frontal eye field (FEF) and V4 simultaneously when monkeys performed a free-gaze visual search task. Saccades were strongly phase-locked to theta oscillations of V4 and FEF local field potentials, and the phase-locking was dependent on saccade direction. The spiking probability of V4 and FEF units was significantly modulated by the theta phase in addition to the time-locked modulation associated with the evoked response. V4 and FEF units showed significantly stronger responses following saccades initiated at their preferred phases. Granger causality and ridge regression analysis showed modulatory effects of theta oscillations on saccade timing. Together, our study suggests phase-locking of saccades to the theta modulation of neural activity in visual and oculomotor cortical areas, in addition to the theta phase locking caused by saccade-triggered responses.

Keywords Visual search · Saccade · Theta rhythm · FEF · V4 · Non-human primate

Introduction

In daily life, primates actively explore the visual world with a systematic pattern of eye movements and fixations. Saccadic eye movements occur every ~ 200 ms–300 ms to draw different parts of the visual environment to the high-acuity fovea for accurate analysis. Active exploratory behaviors are usually associated with theta oscillations in the hippocampus in rodents [1–5] and monkeys [6, 7]. As monkeys perform a recognition memory task, saccades produce a hippocampal theta phase-reset, and enhanced pre-stimulus theta power predicts stronger stimulus encoding [6]. The saccade-related response of theta phase-alignment in the hippocampus is observed during a visual scene search task in human and non-human primates [7]. The visual and oculomotor processes during visual exploration behaviors such as visual search have been studied extensively in the visual cortex [8–16] and association cortex [12, 17–21]. In these cortices, theta oscillations reflect the active neuronal processing of other cognitive operations, such as sustained attention [22–24], learning [25–27], cognitive control [28, 29], decision-making [30], and working memory [31]. Especially in non-human primates, theta oscillations in V4 and the prefrontal cortex (PFC) have been associated with working memory [32, 33]. For example, the phase-locking of single-neuron activity to theta oscillations within V4 and between V4 and PFC was observed while monkeys perform a working memory task

Jin Xie and Ting Yan contributed equally to this work.

Supplementary Information The online version contains supplementary material available at https://doi.org/10.1007/s12264-022-00884-z.

✉ Huihui Zhou
zhouhh@pcl.ac.cn

[1] The Brain Cognition and Brain Disease Institute, Shenzhen Institute of Advanced Technology, Chinese Academy of Sciences, Shenzhen-Hong Kong Institute of Brain Science-Shenzhen Fundamental Research Institutions, Shenzhen 518055, China

[2] University of Chinese Academy of Sciences, Beijing 100049, China

[3] The Research Center for Artificial Intelligence, Peng Cheng Laboratory, Shenzhen 518000, China

[32, 33]. However, the relationship between theta oscillations in the visual and association cortices and visual processing and saccadic behaviors during active visual search is still unclear.

To address this issue, we simultaneously recorded spike and local field potential (LFP) signals in V4 and the frontal eye field (FEF) while monkeys performed a free-gaze visual search task. We found that saccades during the search were strongly phase-locked to theta oscillations of V4 and FEF LFPs, and the phase-locking of saccades to the receptive field (RF) was significantly weaker than those out of the RF. The amplitudes of theta LFP oscillations were far larger than the amplitudes of evoked responses, and the spiking probabilities of neurons were significantly modulated by theta phase. V4 and FEF neurons showed significantly stronger responses following saccades initiated at their preferred phases. Granger causality and ridge regression analysis provided evidence of modulatory effects of theta oscillations on saccade timing. These results suggest the coordination of saccades and neuronal activity of V4 and FEF in the theta rhythm (4 Hz–8 Hz) during visual search.

Materials and Methods

Subjects

This study was carried out with two male rhesus monkeys (*Macaca mulatta* from Xingui Animal Breeding Co., Ltd, Guilin, China) weighing 11 kg–15 kg. Under aseptic conditions, a post to fix the head and two recording chambers were implanted in the heads of each monkey. The two chambers were over the FEF and V4 areas, and were located by magnetic resonance imaging (MRI) before surgery. The visual stimulation and behavioral control were performed using two computers running the Cortex software package (www.cortex.salk.edu). All procedures and animal care were carried out in accordance with the guidelines of the National Care and Use of Animals (China) as approved by the Institutional Animal Care and Use Committee of Shenzhen Institutes of Advanced Technology (approval ID: SIAT-IRB-160223-NS-ZHH-A0187-003).

Visual Stimuli and Behavioral Tasks

Visual stimuli were displayed on a CRT screen (NEC Corporation, Japan) 57 cm from the monkeys' eyes at a resolution of 800 pixels × 600 pixels and a refresh rate of 120 Hz. The stimulus was a combination of one of eight colors and one of eight shapes with a contrast of ~ 1.1° and matched in the number of pixels. For details of matched colors see Zhou and Desimone [34]. A total of 64 different stimuli appeared on a gray background of 14.5 cd/m^2; 20 of 64 stimuli were randomly selected for the search array in a given trial. The target/cue of a given trial was randomly selected from the 20 stimuli.

The researchers trained the monkeys to perform a free-gaze conjunction visual search task. The paradigm is shown in Fig. 1. After center fixation for 400 ms, the screen presented a central cue as the search target, which randomly stayed for 200 ms–2500 ms ("cue period"). Before the search array onset, the monkeys were required to hold fixation within 1.5° of the screen center. Then the screen presented a search array with 20 stimuli, and the central cue was replaced by a center spot at the same time. The monkeys were required to find a target the same as the central cue in the search array within 4000 ms and fixate on it within 2° for 700 ms to receive a drop of juice reward. Before the visual search task, we first used a memory-guided saccade task [34] to determine the cell's receptive field (RF) and stimulus selectivity, with a peripheral stimulus flashed for 100 ms at one of the 20 positions in the above search array.

Recording

With paired recordings in the FEF and V4 areas, we recorded multi-unit spikes and LFPs with a Multichannel Acquisition Processor system from Plexon Inc. (Dallas, USA). Four tungsten microelectrodes (FHC Inc., Bowdoin, USA) passed through the dura mater of each area. The distance between electrodes in an area was 650 μm or 900 μm. To obtain spikes, we filtered the recorded neural signals between 0.25 kHz and 8 kHz, then amplified and digitized them at 40 kHz. The neural signals were filtered between 0.7 Hz and 170 Hz to obtain LFPs. We used MRI imaging to confirm the recorded locations of these two areas, and electrically (< 50 μA) stimulated in the FEF to elicit eye movements. With an infrared eye-tracking system (Eye Link II, SR Research Ltd., Ontario, Canada), we collected eye movements at a sampling rate of 500 Hz while monkeys performed the free-gaze visual search task.

Data Analysis

Data Preprocessing

All data analysis was performed in MatLab (MathWorks, Natick, USA). The recorded sites with a significant visual response (Wilcoxon rank-sum test, $P < 0.05$) were analyzed. Post-stimulus and pre-stimulus periods were chosen for statistical comparisons. The post-stimulus period was 50 ms–250 ms after stimulus onset, and the pre-stimulus period was − 200 ms–0 ms before stimulus onset. The firing rate was calculated by 10-ms non-overlapping bins. The preprocessing of LFPs included powerline artifact

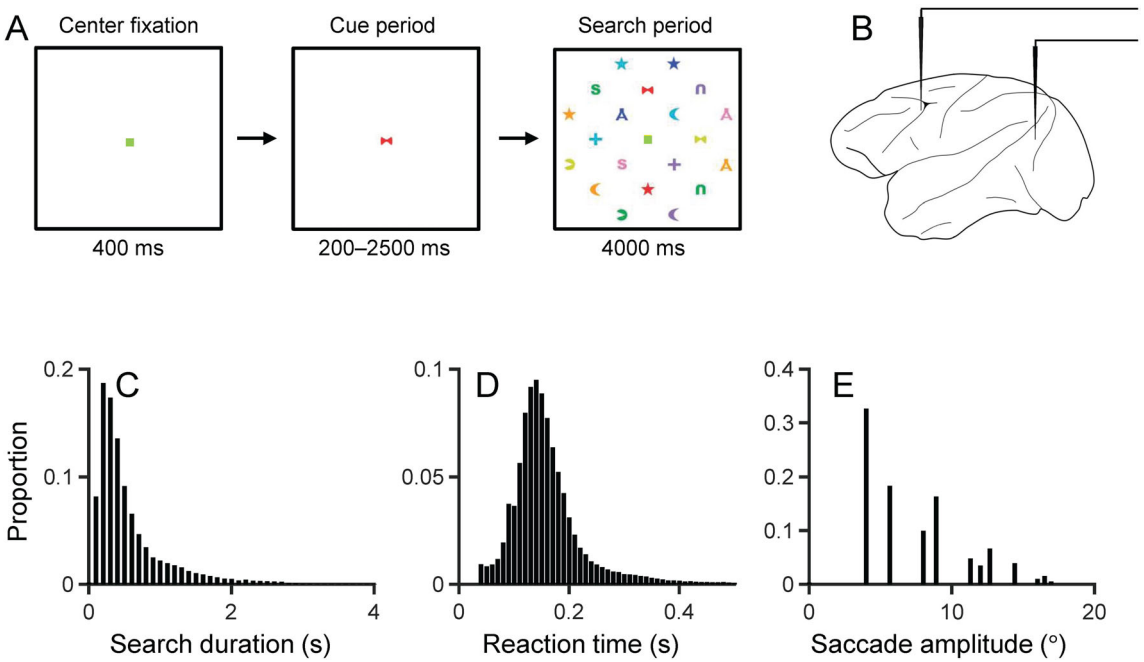

Fig. 1 Task and recording sites. **A** Illustration of the free-gaze conjunction visual search task. No constraints were placed on the search behaviors in order to allow monkeys to conduct the search naturally. **B** Illustration of recording in FEF and V4 areas. Distributions of search durations (**C**), saccade reaction times (**D**), and saccade amplitudes (**E**) during the search.

removal [35] and phase correction [36]. First, we extracted 10-s epoch data containing the point of interest, and calculated the discrete Fourier transform (DFT) at 60 Hz. Based on the amplitudes and phases estimated by DFT, a 60-Hz sine wave was constructed as the estimated power-line artifact, which was subtracted from the 10-s epoch. We corrected the LFP phase shifts caused by the head-stage and preamplifier of the recording system using the utility program provided by Plexon Inc. (FPAlign, http://www.plexoninc.com/support/softwaredownloads.html) as in Gregoriou *et al.* [36]. The sinusoidal signal of 0.5 Hz–400 Hz was injected into two channels. One signal was recorded after the head-stage and preamplifier, and the other was directly injected into the A/D channel without filtering. By Hilbert transform, the average phase difference between these two signals at each frequency was calculated, and the response function of the filter was determined. To eliminate the time delay caused by the original filter, we used an empirical digital filter to reverse the data.

Detection of Significant Theta and Alpha Oscillations in LFPs

LFP signals were band-pass filtered by a finite impulse response (FIR) filter (eegfilt.m from the EEGLAB toolbox). Significant theta oscillations of LFPs during search periods from search array onset to 250 ms after the onset of the last target fixation were detected with a method used in previous studies [37–39]. In short, theta power of LFPs at 4 Hz–8 Hz, and nearby bands of 1 Hz–3 Hz and 9 Hz–14 Hz were calculated. A ratio of $\text{Power}_{4\text{–}8\ \text{Hz}}$/($\text{Power}_{1\text{–}3\ \text{Hz}} + \text{Power}_{9\text{–}14\ \text{Hz}}$) was calculated. We used a ratio threshold of 1.4 to detect significant theta oscillations that gave a clear theta peak in the power spectrum. Significant theta oscillations were detected in V4 LFPs in 35% of search trials, and in FEF LFPs in 17% of trials. Similarly, significant alpha oscillations of LFPs during search periods were detected based on their power (8 Hz–13 Hz) and that of their nearby bands (4 Hz–7 Hz and 14 Hz–16 Hz) using a ratio threshold of 0.8. Significant alpha oscillations were detected in V4 LFPs in 22% of search trials, and in FEF LFPs in 18% of trials.

Saccade Phase-Locking to Theta and Alpha Bands of LFPs

LFP signals were 4 Hz–8 Hz (theta) and band-pass filtered by the FIR filter (eegfilt.m from the EEGLAB toolbox). The Hilbert Transform was applied to the filtered LFP signals to calculate the instantaneous phases of theta oscillations. Saccades that occurred during search periods with significant theta oscillations were used, and phases of theta oscillations of an LFP at the onsets of these saccades were determined, and the distribution with 1° resolution of theta phases at saccade onsets was generated to study the saccade phase-locking to theta oscillations of the LFP.

Saccade onsets were detected based on eye position and velocity signals [40]. We first detected the time when the eye position was 2°–3° away from the averaged fixation position, then traced back to the first time point when the eye position fell within 3×SD of fixation positions from the averaged fixation position. We used this time point as the saccade onset time if the eye movement speed at this time point was also > 30°/s.

To detect significant saccade phase-locking to theta, we performed a Rayleigh analysis using a circular statistics toolbox for MatLab [41]. Given a group of phases ϕ_i (i = 1, …, n), the resultant length of the n phases is the modulus of the first trigonometric moment: $m = \left(\frac{1}{n}\right)\Sigma_{i=1}^{n} e^{j\phi_i}$, where j is the imaginary unit, and e is the natural logarithm base. The theta phase values were transformed before the Rayleigh analysis [42] to exclude the effect of theta wave asymmetry, which leads to a non-uniform phase value distribution. Uniformity of the underlying distribution of phase values (ϕ_U) is particularly desirable for Rayleigh analysis. We devised a transformation : $[-\pi, \pi) \rightarrow [-\pi, \pi)$ such that $\phi_U^{\Psi} = \Psi(\phi_U) = \{\Psi(x)|x \in U\}$ is uniform. Let $F_U : [-\pi, \pi) \rightarrow [0, 1)$ be the empirical cumulative distribution function corresponding to ϕ_U. Then, $\Psi(x) = 2\pi F_U(x) - \pi$ yielded the desired transformation. The Ψ-transformed phase value was used for the Rayleigh analysis. We also calculated the saccade phase-locking to alpha oscillations in LFPs using a similar method. In this analysis, LFP signals were band-pass filtered at 8 Hz–13 Hz. All direct comparisons of phase-locking using resultant length were conducted after equalizing the trial numbers. As a control, saccade phase-locking was also calculated in all search periods with both significant and non-significant oscillations.

To investigate the relationship between saccade behavior and saccade phase-locking, we sorted saccades into saccades to RF and saccades out of RF, and the RF of an LFP was defined as the RF of the unit in the same channel. Phase-locking of these two types of saccade and cross-trial LFP phase consistency [6] around the onset of these two types of saccade were calculated and compared. For cross-trial phase consistency of an LFP, the theta phases of the LFP at each time point within 250 ms around saccade onset were determined, and the distribution of theta phases at each time point was generated. The resultant length based on the theta phase distribution was calculated for each time point to quantify the cross-trial phase consistency of the LFP. Saccades to RF were further sorted into saccades to targets and saccades to distractors. Phase-locking and cross-trial LFP phase consistency in these two conditions were calculated and compared.

Theta Amplitudes in LFP Oscillations and Saccade-Triggered Average Around Saccade Onset

Theta amplitudes of LFP oscillations were calculated on an individual trial base. LFP epochs around saccade onsets were first 4 Hz–8 Hz band-pass filtered. Hilbert Transform was applied to the filtered LFP to calculate the instantaneous theta amplitude in each trial, then the theta amplitudes were averaged across all trials. For theta amplitudes in a saccade-triggered average, LFP epochs around the saccade onset were first averaged across all trials to generate the saccade-triggered average, and a 4 Hz–8 Hz band-pass filter was applied to the saccade-triggered average, then Hilbert Transform was applied to the filtered saccade-triggered average to calculate the instantaneous theta amplitude in the saccade-triggered average. The theta amplitude in a 500-ms window centered on saccade onset was analyzed. We excluded theta amplitude data in the first 200 ms after array onset to avoid the larger LFP response to search array onset, thus, the saccade onsets included in this analysis were at least 450 ms after the array onset. For comparison, we also calculated the theta amplitude in a 500-ms window (− 700 ms to − 200 ms before the array onset) in the cue period with significant theta oscillations, in which monkeys kept central fixation and no saccade was made. As a control, the theta amplitudes were also calculated in all search periods with both significant and non-significant oscillations.

Modulation of Theta Oscillations on Saccades Timing

To investigate the contributions to saccade phase-locking by theta oscillations and the saccade-evoked response, ridge regression and Granger causality were applied for regression and causal tests. LFP epochs around saccade onsets (− 250 ms to + 250 ms, 1-ms bins) were extracted, together with the corresponding theta phases at saccade onsets (see above).

In ridge regression analysis, for each LFP, we took its pre-onset LFPs (LFP_{pre},− 201 ms to − 1 ms), post-onset LFPs (LFP_{post}, 31 ms to 230 ms) around each saccade onset to predict the theta phase at the saccade onset. We also combined LFP_{pre} and LFP_{post} for the prediction. Ridge regression with loss function

$$\mathcal{L}(y, y_{predict}) = \mathrm{MSE}(y, y_{predict}) + \lambda \sum_{i=1}^{m} \theta_i^2$$

was applied, where MSE is the mean square error function, $y_{predict}$ is the prediction from ridge regression, θ_i^2 is the square of the fitting parameters, and λ denotes the parameter for regularization. Five-fold cross-validation

was conducted, and correlation coefficients between the predictions and the real phase values were calculated. Averaged correlation coefficients with SEM across LFP populations were calculated to show the prediction power of pre-onset, post-onset, and the combined LFPs.

Granger causality (GC) analysis was based on the same LFP_{pre}, LFP_{post}, and phases at saccade onsets as used in the regression analysis, and considered them as three sources/targets, indexed by $c = 1, 2, 3$. $c = 1$ for LFP_{pre}, $c = 2$ for LFP_{post}, and $c = 3$ for the phases at saccade onsets. To assess the G-causal influences, we consider c as a target with an observation $A^{(c)}$: $= [A_1^{(c)}, A_2^{(c)}, \ldots, A_T^{(c)}]$. $\mathcal{H}^{(c)}$ denotes the history of the covariates of c, and $\mathcal{H}^{c\setminus\tilde{c}}$ is the history of the covariates of c, excluding the effects of $\tilde{c}$. The log-likelihood ratio statistic associated with the G-causal influence of source ($\tilde{c}$) on target (c) can be defined as

$$\mathcal{F}^{\tilde{c}\to c} = s\left(\omega^{c,\tilde{c}}\right)\log\frac{\mathcal{L}(\omega^{c}|A^{c},\mathcal{H}^{c})}{\mathcal{L}(\omega^{c\setminus\tilde{c}}|A^{c},\mathcal{H}^{c\setminus\tilde{c}})}$$

where ω is a time-varying parameter vector characterizing the underlying dynamics, $\mathcal{L}(\omega|A,\mathcal{H})$ denotes the likelihood of estimated parameter vector ω given the observation sequence A and the history of the covariates $\mathcal{H}$, and $s(\omega) =$ sign(ω). Based on this formulation, the GC effect from source ($\tilde{c}$) to target (c) can be measured as the reduction in the point process log-likelihood of source *($\tilde{c}$)* in the reduced model as compared with the full model. The sign determines the effective excitatory or inhibitory nature of this influence. In our methods, we got the G-causal influence of pre-onset LFPs on theta phases of saccade onsets, and the G-causal influence of post-onset LFPs on theta phases of saccade onsets. For control, we also shuffled the theta phases at saccade onsets across trials and ran significance tests between the original G-causal influences and G-causal influences from shuffled data. LFPs during search periods with significant theta oscillations were included in this analysis.

Influence of Theta and Alpha Oscillations on Spiking of V4 and FEF Units

We analyzed how spiking probability varied with theta phase and the time after saccade onset. In this analysis, LFPs during search periods with significant theta or alpha oscillations were used, and the spikes and LFPs were from the same recording channel. The theta phases of spikes were determined using the same method for determining the phases of saccade onsets (see above). These spike phases were transformed into 0° to 360° and rounded. Spike phase and LFP phase data in the 250-ms epoch after saccade onset were collected. A 250 × 360 matrix was generated with the row number corresponding to the time (0 ms to 249 ms) after saccade onsets and the column number corresponding to the phase value (0° to 359°). We calculated the spiking probability at each time and phase value combination. For example, LFP phases at 100 ms after saccade onset were 20° for 10 times and spikes with 20° phase occurred twice at this time, then the spike probability at this 100 ms and 20° combination was 0.2. If certain phase values never occurred at certain times, spiking probability in these time and phase combinations was set as NaN (not-a-number used in MatLab). Finally, this 250 × 360 spike probability matrix was binned into a 25 × 18 matrix (bin size: 10 ms × 20°) and all NaNs were skipped during this process.

To quantify the spiking probability modulation by theta oscillations, we calculated a modulation index (MI) based on a normalized entropy measure [43, 44]. The spike probabilities in the 250 × 360 matrix were averaged across time with all NaNs skipped and binned into 18 groups based on the phases (20°/bin). The $p(j)$ was the mean spike probability at bin j, and $f(j)$ was given by the following formula:

$$f(j) = \frac{p(j)}{\sum_{j=1}^{N} p(j)} \tag{1}$$

where N represented the total number of bins, and its value was 18. The entropy H was defined by formula 2.

$$H = -\sum_{j=1}^{N} f(j)\log f(j) \tag{2}$$

MI was the normalized entropy, as shown in formula 3.

$$\mathrm{MI} = \frac{H_{\max} - H}{H_{\max}} \tag{3}$$

where $H_{\max}$ represented the maximum possible entropy.

When MI was 0, there was no phase modulation of the spike probability. The higher the MI value, the stronger the phase-probability modulation. After shuffling the spike probability and theta phase, we calculated 200 groups of MI values to analyze the statistical significance of MI. With the permutation distribution of MI values, we determined that the percentage of data points was equal to or greater than the observed MI. The effects of alpha oscillations on the spiking probability of V4 and FEF neurons were also analyzed using similar procedures.

Influence of Phase at Saccade Onset on Spike Response

Based on the distribution of theta phases at saccade onsets, we defined the 60° window where saccades initiated most often as the "preferred phase" of saccades. Another 60° window in which saccades initiated least often was defined

as the "non-preferred phase" of saccades. The distributions of the central values of these preferred phases of V4 and FEF LFPs were generated. We calculated the spike firing rates in a 250-ms window following saccade onset at the preferred phase, non-preferred phase, and all phases. Similarly, the influence of the alpha phase on the spike response was assessed based on the detected significant alpha oscillations. Firing rates in the 250-ms period were binned in 10-ms intervals. For each unit, the firing rate aligned on saccade onset was averaged across trials in the "all saccade phases" condition. All three types of firing rate ("preferred saccade phase", "non-preferred saccade phase", and "all saccade phases") of each unit were normalized to the maximum value of the averaged "all-saccade phases" response during the 250-ms period following saccade onset. Significant differences between firing rates were assessed in the time windows 20 ms–70 ms and 100 ms–150 ms after saccade onset using the Wilcoxon signed-rank test.

To test the influence of phases at saccade onsets on the feature selectivity, we also calculated V4 responses to stimuli with the preferred and non-preferred colors or shapes following saccade onsets at their preferred and non-preferred phases. All four types of firing rates (Fig. 8) in each unit were normalized to the maximum value of the averaged "preferred saccade phase, preferred feature in RF" response during the 250-ms period following saccade onset. In this analysis, the spike signal for calculating firing rate and LFP saccade phase-locking was from the same recording channel. As a control, the influence of phase at saccade onset was also assessed during all search periods with both significant and non-significant oscillations.

Results

We recorded 134 multi-units and LFPs in the FEF area and 136 multi-units and LFPs in the V4 area while the two monkeys performed a free-gaze visual search task (Fig. 1). All multi-units showed significant visual responses (Wilcoxon rank-sum test, $P < 0.05$). The monkeys performed the task at 95% (monkey L) and 98% (monkey G) correct. Figure 1C–E shows the distributions of search duration, reaction time, and saccade amplitude during the search. Figure S1E and F show representative MRI images of the two areas.

Saccade Phase-Locking to the Theta Band in V4 and FEF LFPs

To investigate the relationship between theta oscillations and saccades, we calculated the phases of the theta band in V4 and FEF LFPs at saccade onset. An example of LFP overlaid with its theta (4 Hz–8 Hz) band trace during a search period is illustrated in Fig. 2A along with saccade times and spikes, showing clear theta oscillation in the example LFP. Search periods with significant theta oscillations were determined based on a theta detection method [37–39]. Power spectral analysis of LFPs during these periods revealed a clear peak at theta frequencies (Fig. 2B, F). Figure 2C shows saccade phase-locking to theta oscillations of a V4 LFP. In this example, saccades initiated most often at theta phases around 0° or 360°, but least often at phases around 200°. We ran a Rayleigh analysis on the phase distributions and found that saccades were significantly phase-locked to theta oscillations in 135 of 136 V4 LFPs (averaged resultant length = 0.351 ± 0.0099, $P < 0.05$). Figure 2D shows the distribution of resultant lengths of saccade phase-locking to all 136 V4 LFPs. We also investigated saccade phase-locking to significant alpha oscillations in V4 LFPs. Phase-locking to alpha was significantly weaker than that to theta oscillations in V4 LFPs (Wilcoxon signed-rank test, $P < 0.001$; Fig. 2E). Saccades were also significantly phase-locked to theta oscillations in 132 of 134 FEF LFPs (Fig. 2G, H) and this phase-locking was also significantly stronger than that to FEF alpha oscillations (Wilcoxon signed-rank test, $P < 0.001$; Fig. 2I). Together, these results suggested that the phases of theta oscillations in V4 and FEF were both associated with saccade timing. Similar trends of saccade phase-locking were also found during all search periods with both significant and non-significant oscillations (Fig. S2A, B, D, E). As a control, we also compared saccade phase-locking to oscillations at 3 Hz and 6 Hz–8 Hz, and found stronger saccade phase-locking to 6 Hz–8 Hz oscillations in V4 and FEF (Fig. S6D, H).

To investigate the connection between the saccade phase-locking and exploratory behaviors, we calculated saccade phase-locking to significant theta oscillations (Fig. S3A, D) during inter-trial intervals (ITIs) with a dark screen. Saccade phase-locking during ITIs was significantly weaker than the phase-locking during search periods in V4 and FEF (Fig. S3B, C, E, and F), suggesting a stronger correlation between saccade initiation and theta oscillations during exploratory search.

To further reveal the relationship between LFP theta oscillations and saccade initiations, we calculated 12 LFP traces, with each averaged across LFP epochs with their theta phases at saccade onsets belonging to the same 30° bins (12 bins for 360°), and the saccade-evoked responses were calculated from all LFP epochs (Fig. 2J, K). There were clear theta oscillations in these LFP traces during the pre-onset period, and systematic phase shifts of these LFP traces varied with their theta phase at saccade onset, suggesting that the theta phase at saccade onset was related

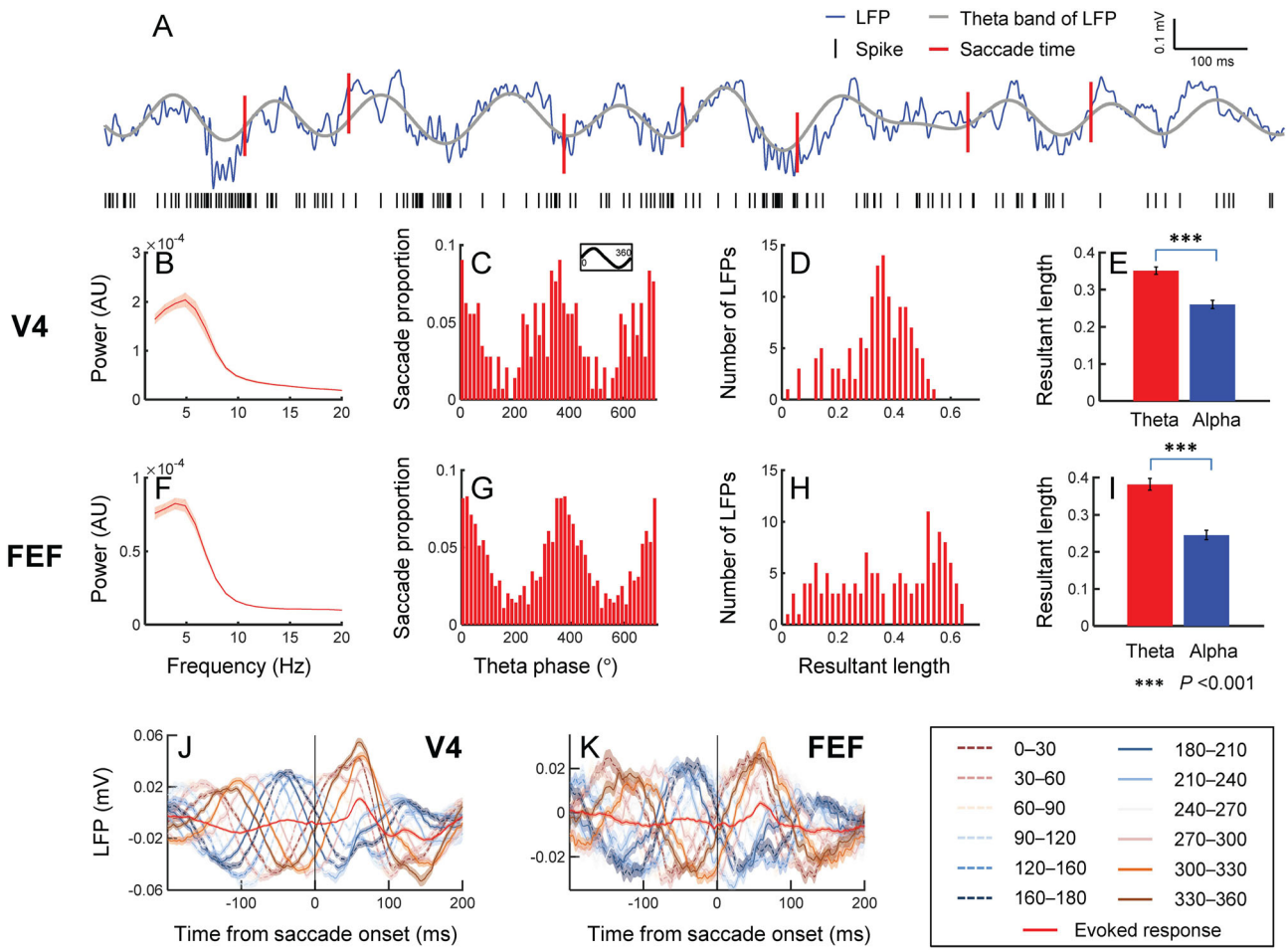

Fig. 2 Saccade phase-locking to the theta band of FEF and V4 LFPs. **A** Raw LFP trace during the search period superimposed on saccade times, and a theta (4 Hz–8 Hz) band-filtered trace of the example LFP. Below: a spike train of a unit recorded simultaneously. **B** Population average of the power spectrum of V4 LFPs during search periods with significant theta oscillations showing a peak at theta frequency. The SEM of the power spectrum across LFPs is marked by shading above and below the average. **C** An example of saccade phase-locking to a V4 LFP with significant theta oscillation. *X*-axis, phase values of theta oscillations at saccade onset; *Y*-axis, proportion of saccades within each phase bin; bin size, 15°. The sinusoid at the top of the panel illustrates a theta cycle. **D** Distribution of resultant lengths quantifying saccade phase-locking to V4 LFPs with significant theta oscillation. *X*-axis, resultant length of saccade phase-locking; *Y*-axis, number of LFPs within each resultant length bin; bin size, 0.02. **E** Saccade phase-locking to significant theta oscillation and phase-locking to significant alpha oscillation (Wilcoxon signed-rank test, $P < 0.001$; $n = 136$) in V4. The SEM of these averages is marked by error bars. **F–I** As in **B–E**, except FEF LFPs ($n = 134$) with significant oscillations. **J** Systematic phase shifts of averaged LFP traces vary with their theta phase at saccade onset. Each trace is averaged across LFP epochs with their theta phase at saccade onset belonging to the same 30° bin (12 bins for 360°). The saccade-evoked response is also shown (red trace), which is averaged across all LFP epochs around saccade onset. **K** As in **J**, except for FEF LFPs with significant theta oscillations.

to the theta oscillation during the pre-onset period. The evoked responses were also smaller than the theta oscillations in the pre-onset period, which could include multiple time-locked components, such as saccade-related activity and the visual response. Similar systematic phase-shifts of theta oscillations also occurred during all search periods with both significant and non-significant theta oscillations (Fig. S2C, F).

In the visual search, monkeys made saccades with an average reaction time of 172.7 ± 0.2 ms (median: 153.0 ms; Fig. 1D). This rhythm of saccades was in the theta range, raising the possibility that theta oscillations during search might be caused by combination of the theta rhythm of saccades and the LFP response time-locked to saccade onset. To test this hypothesis, we compared the amplitude of the theta band of LFPs during the search period, calculated from the LFPs on individual trials, and the amplitude of the theta band in saccade-triggered averages of LFPs, reflected as the LFP response time-locked to saccade onset. If the hypothesis were true, the theta amplitude calculated from the saccade-triggered averages and the theta amplitude calculated from LFPs based on individual trials should be similar. All LFP amplitudes were calculated during search periods with

significant theta oscillations. Figure 3A shows the population averages of the two theta amplitudes of V4 LFPs around the saccade onset. The theta amplitude of saccade-triggered averages was far smaller than the amplitude of theta oscillations of LFPs on individual trials (Fig. 3A, B; Wilcoxon signed-rank test, $P < 0.001$). The former amplitude was just $\sim$ 30% of the latter, suggesting that the theta rhythm of saccades and the LFP response time-locked to saccade onset cannot fully explain the theta oscillations in V4 and FEF LFPs during a search. We obtained similar results in FEF LFPs (Fig. 3C, D). Furthermore, we calculated the amplitude of theta oscillation during the Cue period in which no saccade occurred. We found that the theta amplitude in the Cue period was only slightly weaker than that during the Search period, but far larger than that in the saccade-triggered average in both V4 and FEF (Fig. 3B, D), suggesting that there were ongoing theta oscillations in the two areas independent of the evoked responses during visual search. LFP amplitudes calculated during all search periods with both significant and non-significant oscillations showed similar trends (Fig. S4).

We ran a ridge regression to predict the theta phase value at saccade onset based LFP_{pre} and LFP_{post} (Methods) to investigate two possible hypotheses about the mechanisms of the theta phase-locking of saccades: saccade initiations are modulated by theta oscillations (Hypothesis 1), that is, particular phases of theta oscillations trigger saccades; and saccades reset theta oscillations at specific phases (Hypothesis 2). The mechanisms of phase resetting are considered to be phase concentrations in response to saccades, thus, the resetting process might be more related to LFPs during the post-saccade period with strong evoked responses (and Hypothesis 2). The phase-locking of saccades related to LFP_{pre} might be more linked to Hypothesis 1, where the theta oscillations were obvious and evoked responses were very weak (Figs. 2J, K, 3). We

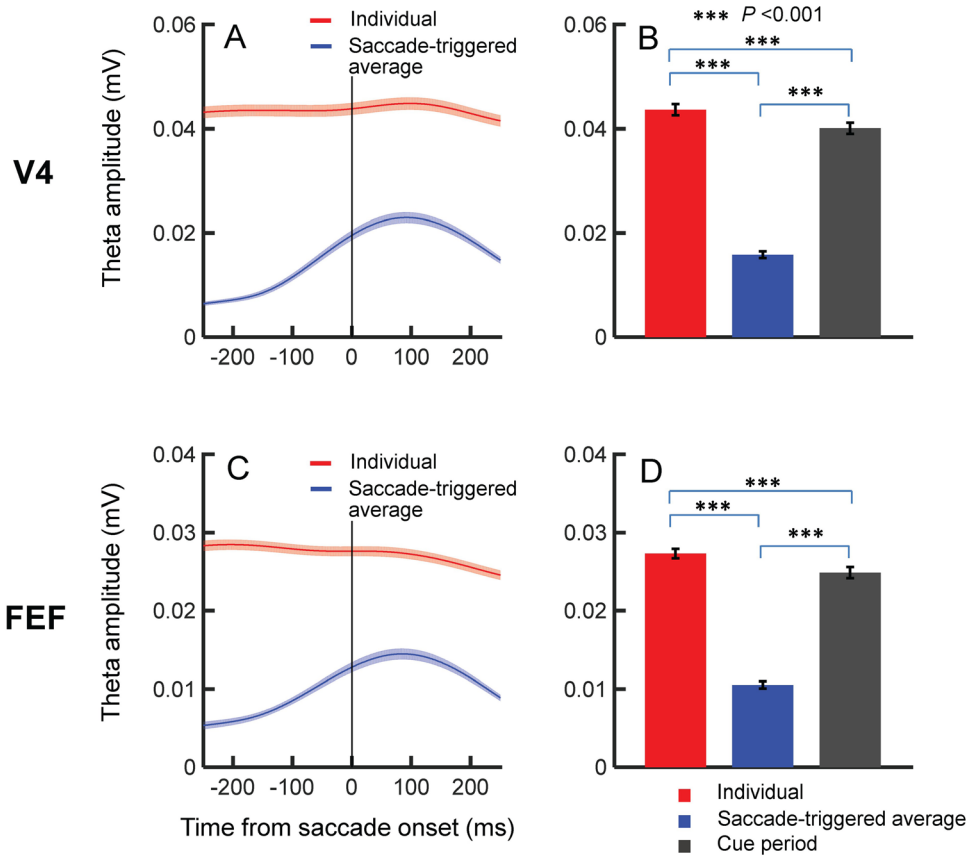

Fig. 3 Amplitudes of theta oscillations around saccade onset. **A** Population averages of amplitudes of V4 LFPs at theta frequencies during search periods with significant theta oscillations. Red line, theta amplitudes on each individual trial were calculated first and then averaged across all trials in all V4 LFPs; blue line, epochs around saccade onsets of an LFP were averaged to generate a saccade onset triggered average of the LFP, and theta amplitude of this saccade-triggered average was calculated, then the theta amplitudes of the saccade-triggered averages were averaged across all V4 LFPs. The SEM of the theta amplitudes is marked by the shading above and below the averages. **B** Averaged theta amplitudes in V4. Gray bar, averaged theta amplitude in a 500-ms window (from 700 ms to 200 ms before search array onset) in Cue periods with significant theta oscillations (Wilcoxon signed-rank test, $P < 0.001$; $n = 136$). The SEM of these averages is marked by error bars. Formats in **C** and **D** are the same as in **A** and **B**, except for FEF LFPs with significant theta oscillations.

used 200-ms pre-onset LFPs and post-onset LFPs to predict the theta phase at saccade onset [45] for comparison. Coefficients between regressed LFP_{pre} and real theta phases were significantly larger than those for LFP_{post} (Fig. 4A, C; V4: Pre-onset, 0.43 ± 0.011, Post-onset, 0.31 ± 0.0086; Pre-onset *vs* Post-onset: Wilcoxon signed-rank test, $P < 0.001$; FEF: Pre-onset, 0.33 ± 0.021, Post-onset, 0.18 ± 0.019; Pre-onset *vs* Post-onset: Wilcoxon signed-rank test, $P < 0.001$), while the coefficient for $LFP_{pre+post}$ was the largest in both V4 and FEF (V4, 0.48 ± 0.0088; FEF, 0.38 ± 0.017), indicating that theta oscillations before saccade onset might influence the theta phases at saccade onset, in addition to the influence of saccade resetting.

To further check the contributions, we applied the Granger causality method [46] to investigate the causal role of pre-onset LFPs and post-onset LFPs in determining the theta phase at saccade onset. We found a significant causal influence of pre-onset LFPs on the theta phases in V4 (Fig. 4B; Pre-onset, 0.25 ± 0.037; Pre-onset *vs* Pre-shuffled, Wilcoxon signed-rank test, $P < 0.001$) and FEF (Fig. 4D; Pre-onset, 0.21 ± 0.034; Pre-onset *vs* Pre-shuffled, Wilcoxon signed-rank test, $P < 0.001$), with the influence of post-onset LFPs excluded in V4 (Fig. 4B; Post-onset, 0.23 ± 0.035; Post-onset *vs* Post-shuffled, Wilcoxon signed-rank test, $P < 0.001$) and FEF (Fig. 4D; Post-onset, 0.19 ± 0.032; Post-onset *vs* Post-shuffled, Wilcoxon signed-rank test, $P < 0.001$). Together, these results suggested both the mechanisms of theta modulation of saccades and the mechanisms of saccade resetting contribute to the saccade phase-locking.

Influence of Behavior on Saccade Phase-Locking

To investigate the effects of behavior on the saccade phase-locking, we compared the theta phase-locking of saccades to the RF and out of the RF. The RF of an LFP was defined as the RF of the unit recorded from the same channel. Search periods with significant theta oscillations were included in this analysis. The theta phase-locking of saccades to the RF was significantly weaker than that out of the RF in V4 (Wilcoxon signed-rank test, $P = 0.002$; Fig. 5A) and FEF (Wilcoxon signed-rank test, $P = 0.04$; Fig. 5E). The LFP cross-trial phase consistencies in the "saccade to RF" condition were significantly lower than those in the "saccade out of RF" condition during the period mainly after the saccade onset in both V4 and FEF (Wilcoxon signed-rank test, $P < 0.05$; Fig. 5B, F).

Further, we compared the theta phase-locking of saccades to a target in the RF and that of saccades to a distractor in the RF. Theta phase-locking of saccades to a

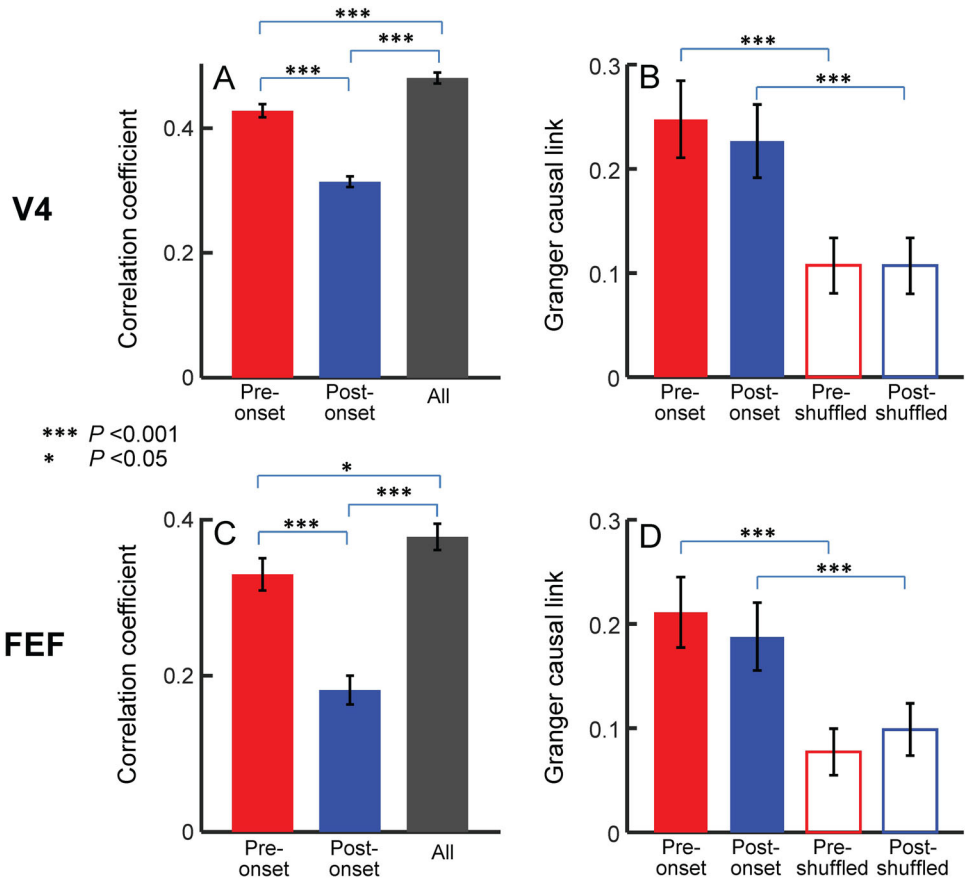

Fig. 4 Modulation of theta oscillations on saccade timing. **A** Predictions of theta phase at saccade onset by V4 LFPs around saccade onset with significant oscillations using ridge regression. Coefficients between experimental theta phase at saccade onset and the predicted theta phase from pre-onset LFPs, post-onset LFPs, and the LFPs with both pre-onset and post-onset LFPs are plotted with significant tests (Wilcoxon signed-rank test, $P < 0.05$; $n = 136$) between all coefficient pairs. **B** Granger causality links from pre-onset LFPs and post-onset LFPs to theta phase at saccade onset, together with links from the LFPs to shuffled theta phases to validate the causality links obtained from experimental data (Wilcoxon signed-rank test, $P < 0.05$; $n = 136$). The SEM of these averages is marked by error bars. **C, D** As in **A** and **B,** except for FEF LFPs with significant theta oscillations (Wilcoxon signed-rank test, $P < 0.05$; $n = 134$).

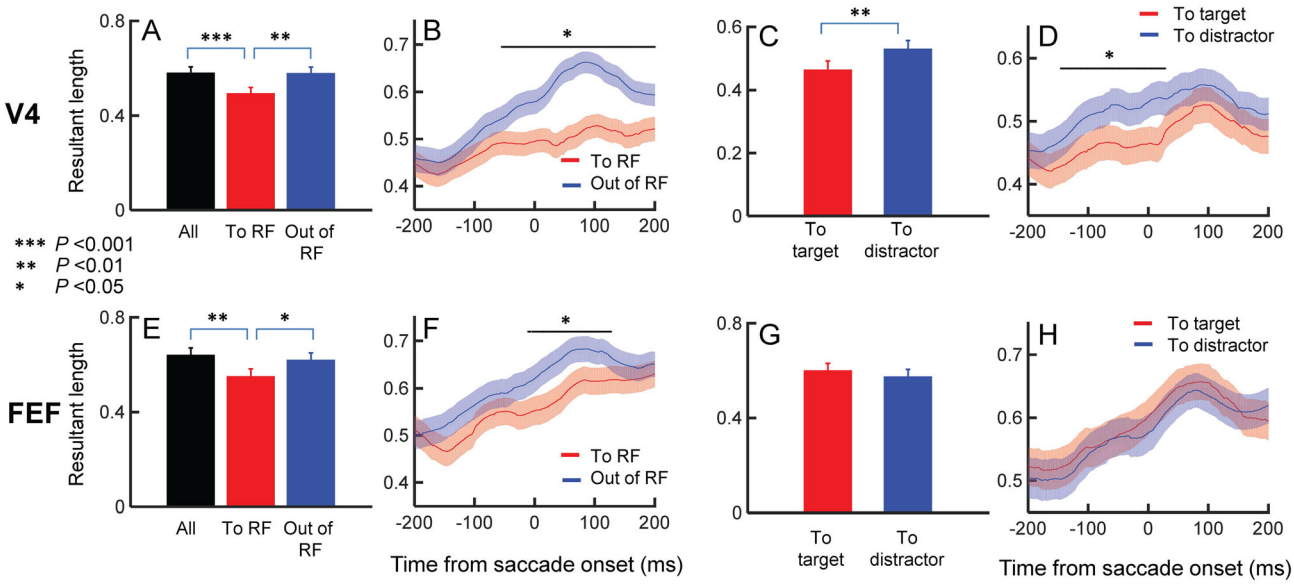

Fig. 5 Influence of behavior on theta phase-locking. **A** V4 theta phase-locking of saccades to the RF, saccades out of the RF, and all saccades during search periods with significant theta oscillations (Wilcoxon signed-rank test, $P < 0.05$; $n = 136$). The SEM of these averages is marked by error bars. **B** Cross-trial theta phase consistency between "saccade to RF" and "saccade out of RF" conditions (Wilcoxon signed-rank test, $P < 0.05$; $n = 136$). The SEM is marked by the shading above and below the averages. **C** V4 theta phase-locking of saccades to a target in the RF and to a distractor in the RF (Wilcoxon signed-rank test, $P < 0.05$; $n = 136$). **D** Cross-trial theta phase consistency between "saccade to target" and "saccade to distractor" conditions (Wilcoxon signed-rank test, $P < 0.05$; $n = 136$). Formats in **E–H** are the same as in **A–D**, except for FEF LFPs during search periods with significant theta oscillations (Wilcoxon signed-rank test, $P < 0.05$; $n = 134$).

target was significantly weaker than that to a distractor in V4 (Wilcoxon signed-rank test, $P = 0.006$; Fig. 5C), but no significant difference was found in the FEF (Fig. 5G). The V4 LFP cross-trial phase consistency in the "saccade to target" condition was also significantly lower during the short period mainly before saccade onset (Wilcoxon signed-rank test, $P < 0.05$; Fig. 5D), while the FEF LFP cross-trial phase consistency was similar in the two conditions (Fig. 5H). Together, the theta phase-locking and phase consistency were more dependent on saccade behaviors (to the RF *vs* out of the RF), than on task-related properties of stimuli in the RF (target *vs* distractor).

Spiking Probability of V4 and FEF Neurons Varies with the Phase of Theta Oscillation

Previous studies have shown that the spiking probabilities of V4 and PFC neurons vary with the phases of theta oscillations in each area [32, 33]. In visual searching, neural responses time-locked to saccade onsets, such as saccade-related activity and visual responses, have effects on spiking probability at theta rhythm, which could confound spiking probability modulation associated with theta oscillations. To dissociate spiking probability changes associated with theta oscillations and the change-associated factors time-locked to saccade onset, we calculated a spiking probability matrix with its rows aligned on the time from saccade onset and its columns aligned on the phase of theta oscillation. Thus, the spiking probability changes related to time-locked factors were revealed along the *Y*-axis, and spiking probability changes related to theta oscillations were revealed along the *X*-axis. Search periods with significant theta oscillation were included in this analysis. The population average of V4 spiking probability varied with the V4 theta phase and the time after saccade onset (Fig. 6A). A peak probability occurred at $\sim$ 100 ms after saccade onset, which might reflect the influence of a time-locked evoked response. The V4 spiking probability also varied with the theta phase, which was high at phases $\sim$ 200° and low at phases between 0° and 100°, suggesting that V4 spiking probability can be modulated by V4 theta oscillations. More importantly, these probability changes associated with the theta phases were evident throughout the whole 250 ms period after saccade onset. We calculated the MI [43] to quantify the theta modulation of spiking probability in different periods after saccade onset. Figure 6B shows the averaged MIs in these periods. Theta modulation was significant in at least 78% of 136 V4 sites in different periods within the 250-ms period after saccade onset (permutation test, $P < 0.05$). Examples of MIs and shuffled MI distributions were illustrated in Fig. S5G, H. We also calculated the spiking probability changes associated with V4 alpha oscillations, but the alpha modulation was significantly weaker than the theta modulation in all

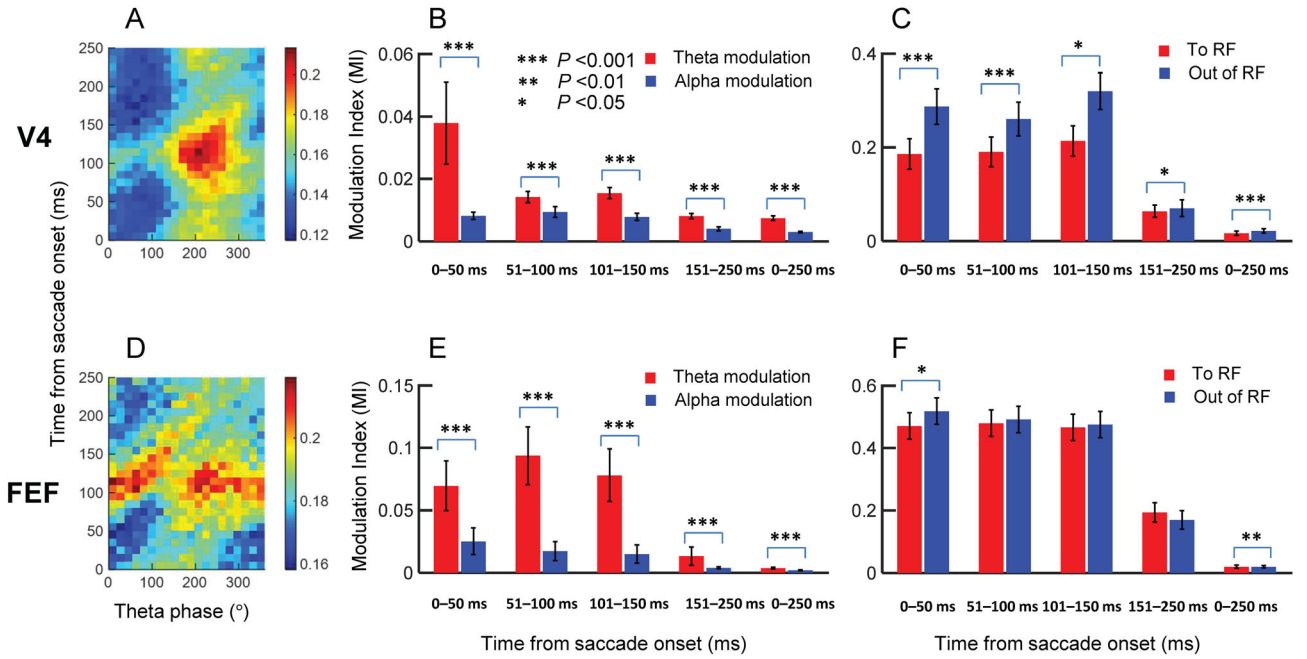

Fig. 6 Spike probability of V4 and FEF units varies with theta phase. **A** Color map of population averages of V4 spike probability that vary with the theta phase and the time from saccade onset. The unit of the scale bar is the mean spike count within 10 ms × 18° bins. *X*-axis, theta phase; *Y*-axis, time from saccade onset. **B** Averaged modulation indexes (MIs) that quantify V4 spiking probability modulated by V4 theta and alpha oscillations in different post-onset periods (Wilcoxon signed-rank test, $P < 0.05$; $n = 136$). Red bars, averaged MIs of theta modulation; blue bars, averaged MIs of alpha modulation. The SEMs of these averages are marked by error bars. **C** Comparison of theta MIs in "saccade to RF" and "saccade out of RF" conditions (Wilcoxon signed-rank test, $P < 0.05$; $n = 136$). **D–F** as in **A–C**, except for spikes and LFPs in the FEF during search periods with significant oscillations (Wilcoxon signed-rank test, $P < 0.05$; $n = 134$).

periods after saccade onset (Wilcoxon signed-rank test, $P < 0.001$; Fig. 6B). In the FEF, the preferred theta phase for spiking varied with time after saccade onset, while this variation was smaller in V4 (Fig. 6A *vs* D). Because the distribution of the preferred theta phase of FEF LFPs at saccade onset showed two peaks (see below and Fig. S2G), we also calculated the theta modulation of spiking probability separately in the two groups of LFPs (Fig. S5I, J), which showed the influence of the preferred phase for saccade onset on the theta modulation of spiking. In the FEF, spiking probability also varied with the phase of theta oscillations throughout the 250-ms period after saccade onset (Fig. 6D, E), which were significant in at least 32% of 134 FEF sites in different periods within the 250-ms period after saccade onset (permutation test, $P < 0.05$). This theta modulation was also significantly stronger than the modulation by FEF alpha oscillations (Wilcoxon signed-rank test, $P < 0.001$; Fig. 6E). The theta modulation of spiking probability was also significant throughout the 250-ms period after saccade onset during all search periods with both significant and non-significant theta oscillations (Fig. S5A, B, D, E).

Theta modulation of spiking was stronger in the "saccade out of RF" condition than in the "saccade to RF" condition in V4 (Wilcoxon signed-rank test, $P < 0.001$ at 0 ms–50 ms, 51 ms–100 ms, 0 ms–250 ms, and $P = 0.02$, 0.03 at 101 ms–150 ms and 151 ms–250 ms; Figs. 6C, S5C), while the theta modulation was similar under these two conditions in the FEF (Figs. 6F, S5F). As a control, we also calculated the modulation of spiking by oscillations at 3 Hz and 6 Hz–8 Hz. The modulation by oscillations at 3 Hz tended to be weaker in V4, but stronger in the FEF (Figs. S6A–C, S6E–G).

Influence of Phase at Saccade Onset on Spike Responses in the FEF and V4

Saccades selectively initiated more often at certain theta phases and spike probability varied with theta phases, suggesting that spike activity following saccade onset might be influenced by the theta phase at saccade onset. To address this, we defined a 60° window of theta phases in which saccades initiated most often as the "preferred phase" of saccades. Another 60° window in which saccades initiated least often was defined as the "non-preferred phase" of saccades. The distributions of the central values of these preferred phases for V4 and FEF LFPs showed shifts between the peaks of the two distributions and a small second peak in the FEF distributions (Fig. S2G). Search periods with significant theta

oscillations were included in this analysis. Figure 7A shows population averages of V4 responses following saccade onsets with different theta phases. Following saccades initiated at their preferred theta phase, V4 activity first decreased, then showed a strong phasic response. At the same time, the averaged LFP traces in these trials increased to a peak around 50 ms after saccade onset (Fig. S7A, red traces), and then decreased sharply. The peak time of this phasic response was ~ 100 ms after the saccade onset indicating that this activity mainly represented the visual response. Following saccades initiated at their non-preferred theta phase, V4 activity stayed at a relatively high level in the early period after saccade onset, while LFP traces decreased in this early period (Fig. S7A, blue trace). In the early period, V4 activity after saccade onsets with non-preferred phases was significantly higher than the activity after saccade onsets with preferred phases (Wilcoxon signed-rank test, $P < 0.001$), However, the latter V4 activity showed a significantly stronger phasic response between 100 ms and 150 ms after saccade onset (Wilcoxon signed-rank test, $P < 0.001$). In the FEF, we only found the effect of theta phase at saccade onset in the early period after the onset (Fig. 7C). We also analyzed the effects of alpha oscillations (Fig. 7B, D), which were weaker than the effects of theta oscillations. The influence of phase at saccade onset on spike responses in the FEF and V4 also occurred in all search periods with both significant and non-significant theta oscillations (Fig. S8A–D). Together, saccade initiations at preferred theta phases might help V4 neurons to give a strong response to the visual stimulus, and establish an optimal condition for stimulus sampling in a visual search.

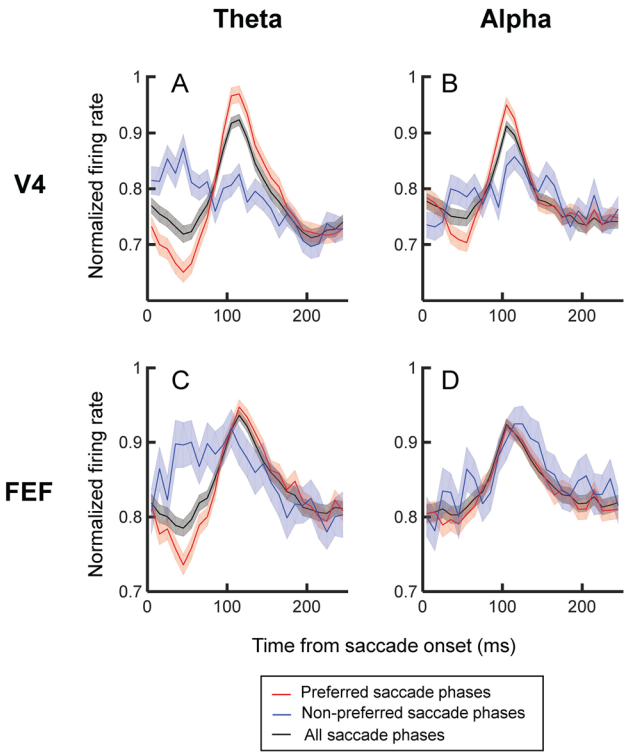

Fig. 7 Influence of phase at saccades onset on responses in V4 and the FEF. **A** Population averages of V4 responses following saccade onset at different theta phases of LFPs with significant theta oscillations. The SEMs of the responses are marked by the shading above and below the averages. **B** Population averages of V4 responses following saccade onset at different alpha phases of LFPs with significant alpha oscillation in V4. **C, D** as in **A** and **B**, except for spikes and LFPs in the FEF with significant oscillations.

Influence of Saccade Phase on Color and Shape Selectivity in V4

We mapped the color and shape selectivity of V4 neurons in the memory-guided saccade task. 79 and 73 V4 neurons showed significant color selectivity and shape selectivity [one-way analysis of variance (ANOVA), $P < 0.05$], respectively. Figure 8A shows averaged responses of the color-selective neurons in a visual search. Search periods with significant theta oscillations were included in this analysis. Following saccade onset with preferred and non-preferred theta phases, these neurons gave significantly stronger responses to stimuli with preferred colors than to stimuli with non-preferred colors. Thus, the color selectivity was retained in these neurons following saccades initiated at different phases. The shape selectivity was also retained (Fig. 8B). Therefore, the theta phase at saccade onset influences the amplitude of spiking rate responses, but not the feature selectivity in V4. Feature selectivity was also maintained following saccades initiated at preferred and non-preferred phases during all search periods with both significant and non-significant theta oscillations (Fig. S8E, F).

Discussion

In this study, we found that saccades were strongly phase-locked to theta oscillations in both V4 and FEF LFPs during a free-gaze visual search. Theta phase-locking of saccades to the RF was significantly weaker than out of the RF. The amplitudes of LFP theta oscillations were far larger than the amplitudes of saccade-evoked responses, supporting the existence of components of theta oscillations in the two areas independent of the evoked responses. The spiking probability of V4 and FEF neurons was significantly modulated by theta oscillations, which could be disassociated from the modulation caused by the evoked responses. V4 neurons showed a significantly stronger evoked response following saccades initiated at their preferred theta phase than that following saccades initiated at their non-preferred phases. In addition to the effects on

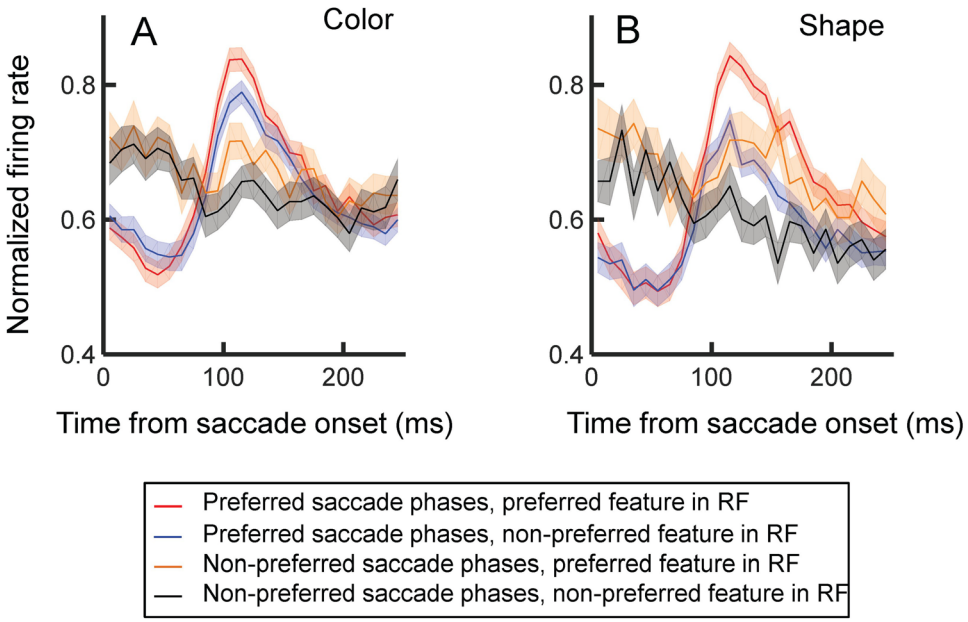

Fig. 8 Influence of theta phase at saccade onset on the color and shape selectivity of V4 units. **A** Influence on color selectivity. Red and blue lines, averaged responses to preferred and non-preferred colors at the preferred theta phase, respectively; orange and black lines, averaged responses to preferred and non-preferred colors at the non-preferred theta phase, respectively. **B** Influence on shape selectivity. Formats are the same as in **A**, except for preferred and non-preferred shapes. All the above analyses were performed during search periods with significant theta oscillations.

saccade phase-locking by saccade-evoked responses, Granger causality and ridge regression analysis provided evidence of modulatory effects of theta oscillations on saccade timing. These results suggested that saccades and neuronal activity in V4 and the FEF are coordinated at theta rhythm (4 Hz–8 Hz) during active visual exploration.

We found strong saccade phase-locking to theta oscillations, theta modulation of spiking activity, systematic phase shifts of theta oscillations varied with their theta phases at saccade onset, and an increase of cross-trial phase consistency during the post-onset period in both V4 and the FEF, while there were also differences in the effects of saccades on the theta phase-locking, distribution of preferred theta phases at saccade onset, and relationships between modulation by oscillations at 3 Hz and 6 Hz–8 Hz on spiking in the two areas. These results might be related to the overlap and distinct functions of V4 and the FEF in visual searching. We recorded a drop in firing rate in the early period following a saccade initiated at its preferred theta phase and a high firing rate following a saccade initiated at its non-preferred phase, while the LFPs showed the opposite changes during the same period. The opposite changes in firing rate and LFP signals are consistent with recent studies [47, 48]. It was likely that different time courses of LFPs might result in different theta phase values, then were associated with different firing rate patterns. In the FEF, the preferred theta phase for spiking varied clearly with the time after saccade onset, while these preferred phase jitters in theta modulation of spiking were weaker in V4, suggesting different levels of time-dependent modulation of the theta modulation of spiking in the two areas. The interactions between the two types of modulation are still not clear, so further studies are needed to understand these interactions.

Theta Modulation of Saccade Timing

Theta oscillations associated with active exploratory behaviors have been studied extensively in the hippocampus and the medial prefrontal cortex of rodents [1–5, 42, 49]. In non-human primates, previous studies have shown phase-alignment and phase-resetting of hippocampal theta-frequency oscillations caused by saccades during visual exploratory behaviors [6, 7, 50, 51]. Hoffman *et al*. [7] found theta phase alignment of saccades during active searching, but not during ITIs with a dark screen. Consistently, we recorded stronger saccade phase-locking during the search period than during ITIs in V4 and the FEF (Fig. S3C, F).

We found similar theta amplitudes before and after saccade onset (Fig. 3A, C) and enhancement of cross-trial phase consistency following saccade onset (Fig. 5B, D, F, H), consistent with previous findings that support the hypothesis of saccade resetting of theta oscillations [6, 7, 51, 52]. The saccade phase-locking in our studies could be caused by this resetting mechanism. However, we recorded evident theta oscillations in the averaged LFP traces during the pre-onset period, whose phases shifted systematically with their theta phase at saccade onset, suggesting that the theta phase at saccade onset is related to the theta oscillations of this period. Consistent with this, the evoked response and cross-trial LFP phase consistency were also clearly weaker in this period than the response and consistency during the post-onset period. Ridge

regression analysis further showed significantly higher correlation coefficients between the real and predicted theta phase at saccade onset based on the LFP_{pre} than the coefficients based on the LFP_{post}, which suggested a better prediction of the theta phase based on the pre-onset LFP, indicating that the evoked response during the pre-onset period cannot explain the correlation between pre-onset LFP and the theta phase at saccade onset. In addition, Granger causality analysis showed a significant causal influence of pre-onset LFP on the theta phase at saccade onset as the influence of the post-onset LFP was excluded. In this method, to test the causal link from one source to the target, the prediction from all sources without that single source is compared with the prediction from all sources to find the significant causal influence of the single source. This causality result suggested that pre-onset theta oscillations might play an important role in determining the phase at saccade onset. Together, our study supported the hypothesis that both pre-onset and post-onset LFPs contribute to the saccade phase-locking, while also providing evidence for theta oscillation modulation of saccade timing.

Theta Oscillations and Visual Attention

Theta oscillations have also been associated with the fluctuations of covert spatial attention in a number of recent studies [53–61], involving mechanisms such as theta phases in the lateral intraparietal area and FEF acting as a clocking mechanism to organize alternating attentional states [54], coordinating theta-rhythmic attention states through pulvino-cortical interactions [59], and theta oscillations and coupling in V1 and V4 [61]. Spyropoulos *et al.* [61] showed stronger coherence of LFPs within V4 when the stimulus in RF is not attended. Consistent with this, we found stronger theta cross-trial phase consistency in the "saccade out of RF" condition in V4. In addition, the stronger theta modulation of spiking in V4 and the FEF in the "saccade out of RF" condition found in this study are consistent with the finding that spike-field coherence of low frequencies including theta is desynchronized with attention within the V4 and FEF areas [36, 62]. We also found a weak difference in theta cross-trial phase consistency in V4 between "saccade to target" and "saccade to distractor" conditions and no significant difference in the FEF. This might be related to the fact that monkeys can make multiple saccades to find the target and the "saccade to distractor" condition did not result in search errors in most trials, compared with tasks with only one saccade allowed in a search trial, which might weaken the difference between the two types of condition.

We extended the study of theta oscillations in the visual cortex and FEF to active visual exploration with rhythmic saccades or overt spatial attention shifts. Our results of saccade phase-locking to theta oscillations together with ridge regression and Granger causality analysis suggested that theta oscillations participate in the timing of saccades or overt spatial attention shifts during active visual exploration.

Acknowledgements We are grateful for the financial support from the National Natural Science Foundation of China (31671108 and 31800900), the National Key R&D Program of China (2017YFC1307500), the Shenzhen Science and Technology Innovation Commission (JCYJ20180508152240368) and the Shenzhen Basic Research Program (JCYJ20200109114805984).

Conflict of interest The authors declare that they have no conflict of interest.

References

1. Buzsáki G. Theta oscillations in the hippocampus. Neuron 2002, 33: 325–340.
2. Buzsáki G. Theta rhythm of navigation: Link between path integration and landmark navigation, episodic and semantic memory. Hippocampus 2005, 15: 827–840.
3. Grastyan E, Lissak K, Madarasz I, Donhoffer H. Hippocampal electrical activity during the development of conditioned reflexes. Electroencephalogr Clin Neurophysiol 1959, 11: 409–430.
4. Vanderwolf CH. Hippocampal electrical activity and voluntary movement in the rat. Electroencephalogr Clin Neurophysiol 1969, 26: 407–418. https://doi.org/10.1016/0013-4694(69)90092-3.
5. Winson J. Patterns of hippocampal Theta rhythm in the freely moving rat. Electroencephalogr Clin Neurophysiol 1974, 36: 291–301. https://doi.org/10.1016/0013-4694(74)90171-0.
6. Jutras MJ, Fries P, Buffalo EA. Oscillatory activity in the monkey hippocampus during visual exploration and memory formation. Proc Natl Acad Sci U S A 2013, 110: 13144–13149.
7. Hoffman KL, Dragan MC, Leonard TK, Micheli C, Montefusco-Siegmund R, Valiante TA. Saccades during visual exploration align hippocampal 3–8 Hz rhythms in human and non-human Primates. Front Syst Neurosci 2013, 7: 43.
8. Bartlett AM, Ovaysikia S, Logothetis NK, Hoffman KL. Saccades during object viewing modulate oscillatory phase in the superior temporal sulcus. J Neurosci 2011, 31: 18423–18432.
9. Bichot NP, Rossi AF, Desimone R. Parallel and serial neural mechanisms for visual search in macaque area V4. Science 2005, 308: 529–534.
10. Chelazzi L, Duncan J, Miller EK, Desimone R. Responses of neurons in inferior temporal cortex during memory-guided visual search. J Neurophysiol 1998, 80: 2918–2940.
11. Mazer JA, Gallant JL. Goal-related activity in V4 during free viewing visual search: Evidence for a ventral stream visual salience map. Neuron 2003, 40: 1241–1250. https://doi.org/10.1016/S0896-6273(03)00764-5.
12. Monosov IE, Sheinberg DL, Thompson KG. Paired neuron recordings in the prefrontal and inferotemporal cortices reveal that spatial selection precedes object identification during visual search. Proc Natl Acad Sci U S A 2010, 107: 13105–13110.
13. Mruczek REB, Sheinberg DL. Activity of inferior temporal cortical neurons predicts recognition choice behavior and recognition time during visual search. J Neurosci 2007, 27: 2825–2836.

14. Ogawa T, Komatsu H. Target selection in area V4 during a multidimensional visual search task. J Neurosci 2004, 24: 6371–6382.
15. Schiller PH, Lee K. The role of the primate extrastriate area V4 in vision. Science 1991, 251: 1251–1253.
16. Hu Q, Hu W, Liu K, Bu X, Hu L, Li L. Modulation of spike count correlations between macaque primary visual cortex neurons by difficulty of attentional task. Neurosci Bull 2021, 2021: 1–16.
17. Buschman TJ, Miller EK. Top-down versus bottom-up control of attention in the prefrontal and posterior parietal cortices. Science 2007, 315: 1860–1862.
18. Hasegawa RP, Matsumoto M, Mikami A. Search target selection in monkey prefrontal cortex. J Neurophysiol 2000, 84: 1692–1696.
19. Ipata AE, Gee AL, Goldberg ME, Bisley JW. Activity in the lateral intraparietal area predicts the goal and latency of saccades in a free-viewing visual search task. J Neurosci 2006, 26: 3656–3661.
20. Schall JD, Hanes DP. Neural basis of saccade target selection in frontal eye field during visual search. Nature 1993, 366: 467–469.
21. Thomas NWD, Paré M. Temporal processing of saccade targets in parietal cortex area LIP during visual search. J Neurophysiol 2007, 97: 942–947.
22. Clayton MS, Yeung N, Cohen Kadosh R. The roles of cortical oscillations in sustained attention. Trends Cogn Sci 2015, 19: 188–195. https://doi.org/10.1016/j.tics.2015.02.004.
23. Sellers KK, Yu CX, Zhou ZC, Stitt I, Li YH, Radtke-Schuller S, *et al*. Oscillatory dynamics in the frontoparietal attention network during sustained attention in the ferret. Cell Rep 2016, 16: 2864–2874.
24. Han HB, Lee KE, Choi JH. Functional dissociation of theta oscillations in the frontal and visual cortices and their long-range network during sustained attention. eNeuro 2019, https://doi.org/10.1523/ENEURO.0248-19.2019.
25. Chen H, Wang YJ, Yang L, Sui JF, Hu ZA, Hu B. Theta synchronization between medial prefrontal cortex and cerebellum is associated with adaptive performance of associative learning behavior. Sci Rep 2016, 6: 20960.
26. Zold CL, Hussain Shuler MG. Theta oscillations in visual cortex emerge with experience to convey expected reward time and experienced reward rate. J Neurosci 2015, 35: 9603–9614.
27. Levy JM, Zold CL, Namboodiri VMK, Hussain Shuler MG. The timing of reward-seeking action tracks visually cued Theta oscillations in primary visual cortex. J Neurosci 2017, 37: 10408–10420.
28. Cavanagh JF, Frank MJ. Frontal theta as a mechanism for cognitive control. Trends Cogn Sci 2014, 18: 414–421.
29. Chen JZ, Wang Q, Li NX, Huang SJ, Li M, Cai JB, *et al*. Dyskinesia is closely associated with synchronization of theta oscillatory activity between the substantia nigra pars reticulata and motor cortex in the off L-dopa state in rats. Neurosci Bull 2021, 37: 323–338.
30. Meindertsma T, Kloosterman NA, Nolte G, Engel AK, Donner TH. Multiple transient signals in human visual cortex associated with an elementary decision. J Neurosci 2017, 37: 5744–5757.
31. Sauseng P, Griesmayr B, Freunberger R, Klimesch W. Control mechanisms in working memory: A possible function of EEG theta oscillations. Neurosci Biobehav Rev 2010, 34: 1015–1022.
32. Lee H, Simpson GV, Logothetis NK, Rainer G. Phase locking of single neuron activity to theta oscillations during working memory in monkey extrastriate visual cortex. Neuron 2005, 45: 147–156.
33. Liebe S, Hoerzer GM, Logothetis NK, Rainer G. Theta coupling between V4 and prefrontal cortex predicts visual short-term memory performance. Nat Neurosci 2012, 15: 456–462, S1-2.
34. Zhou HH, Desimone R. Feature-based attention in the frontal eye field and area V4 during visual search. Neuron 2011, 70: 1205–1217.
35. Fries P, Womelsdorf T, Oostenveld R, Desimone R. The effects of visual stimulation and selective visual attention on rhythmic neuronal synchronization in macaque area V4. J Neurosci 2008, 28: 4823–4835.
36. Gregoriou GG, Gotts SJ, Zhou HH, Desimone R. High-frequency, long-range coupling between prefrontal and visual cortex during attention. Science 2009, 324: 1207–1210.
37. Schomburg EW, Fernández-Ruiz A, Mizuseki K, Berényi A, Anastassiou CA, Koch C, *et al*. Theta phase segregation of input-specific gamma patterns in entorhinal-hippocampal networks. Neuron 2014, 84: 470–485.
38. Montgomery SM, Sirota A, Buzsáki G. Theta and gamma coordination of hippocampal networks during waking and rapid eye movement sleep. J Neurosci 2008, 28: 6731–6741.
39. Csicsvari J, Hirase H, Czurkó A, Mamiya A, Buzsáki G. Oscillatory coupling of hippocampal pyramidal cells and interneurons in the behaving Rat. J Neurosci 1999, 19: 274–287.
40. Schall JD, Hanes DP, Thompson KG, King DJ. Saccade target selection in frontal eye field of macaque. I. Visual and premovement activation. J Neurosci 1995, 15: 6905–6918.
41. Berens P. CircStat: AMATLABToolbox for circular statistics. J Stat Soft 2009, 31: 1–21. https://doi.org/10.18637/jss.v031.i10.
42. Siapas AG, Lubenov EV, Wilson MA. Prefrontal phase locking to hippocampal theta oscillations. Neuron 2005, 46: 141–151.
43. Tort ABL, Kramer MA, Thorn C, Gibson DJ, Kubota Y, Graybiel AM, *et al*. Dynamic cross-frequency couplings of local field potential oscillations in rat striatum and hippocampus during performance of a T-maze task. Proc Natl Acad Sci U S A 2008, 105: 20517–20522.
44. Hurtado JM, Rubchinsky LL, Sigvardt KA. Statistical method for detection of phase-locking episodes in neural oscillations. J Neurophysiol 2004, 91: 1883–1898.
45. Marquardt DW, Snee RD. Ridge regression in practice. Am Stat 1975, 29: 3–20. https://doi.org/10.2307/2683673.
46. Sheikhattar A, Miran SN, Liu J, Fritz JB, Shamma SA, Kanold PO, *et al*. Extracting neuronal functional network dynamics via adaptive Granger causality analysis. Proc Natl Acad Sci U S A 2018, 115: E3869–E3878.
47. Confais J, Malfait N, Brochier T, Riehle A, Kilavik BE. Is there an intrinsic relationship between LFP beta oscillation amplitude and firing rate of individual neurons in macaque motor cortex? Cereb Cortex Commun 2020, 1: tgaa017.
48. Bellay T, Shew WL, Yu S, Falco-Walter JJ, Plenz D. Selective participation of single cortical neurons in neuronal avalanches. Front Neural Circuits 2021, 14: 620052.
49. Lubenov EV, Siapas AG. Hippocampal theta oscillations are travelling waves. Nature 2009, 459: 534–539.
50. Courellis HS, Nummela SU, Metke M, Diehl GW, Bussell R, Cauwenberghs G, *et al*. Spatial encoding in primate hippocampus during free navigation. PLoS Biol 2019, 17: e3000546.
51. Meister MLR, Buffalo EA. Getting directions from the hippocampus: The neural connection between looking and memory. Neurobiol Learn Mem 2016, 134: 135–144.
52. Killian NJ, Potter SM, Buffalo EA. Saccade direction encoding in the primate entorhinal cortex during visual exploration. Proc Natl Acad Sci U S A 2015, 112: 15743–15748.
53. Fiebelkorn IC, Saalmann YB, Kastner S. Rhythmic sampling within and between objects despite sustained attention at a cued location. Curr Biol 2013, 23: 2553–2558.
54. Fiebelkorn IC, Pinsk MA, Kastner S. A dynamic interplay within the frontoparietal network underlies rhythmic spatial attention. Neuron 2018, 99: 842-853.e8.

55. Helfrich RF, Fiebelkorn IC, Szczepanski SM, Lin JJ, Parvizi J, Knight RT, *et al*. Neural mechanisms of sustained attention are rhythmic. Neuron 2018, 99: 854-865.e5.
56. Landau AN, Fries P. Attention samples stimuli rhythmically. Curr Biol 2012, 22: 1000–1004.
57. Busch NA, VanRullen R. Spontaneous EEG oscillations reveal periodic sampling of visual attention. Proc Natl Acad Sci U S A 2010, 107: 16048–16053.
58. VanRullen R, Carlson T, Cavanagh P. The blinking spotlight of attention. Proc Natl Acad Sci U S A 2007, 104: 19204–19209.
59. Fiebelkorn IC, Pinsk MA, Kastner S. The mediodorsal pulvinar coordinates the macaque fronto-parietal network during rhythmic spatial attention. Nat Commun 2019, 10: 215.
60. Landau AN, Schreyer HM, van Pelt S, Fries P. Distributed attention is implemented through theta-rhythmic gamma modulation. Curr Biol 2015, 25: 2332–2337.
61. Spyropoulos G, Bosman CA, Fries P. A theta rhythm in macaque visual cortex and its attentional modulation. Proc Natl Acad Sci U S A 2018, 115: E5614–E5623.
62. Yan T, Zhou HH. Synchronization between frontal eye field and area V4 during free-gaze visual search. Zool Res 2019, 40: 394–403.